World Academy of Science, Engineering and Technology
International Journal of Environmental and Ecological Engineering
Vol:15, No:6, 2021

Two-Dimensional Modeling of Seasonal Freeze and Thaw in an Idealized River Bank

Jiajia Pan, Hung Tao Shen

***Abstract*—**Freeze and thaw occurs seasonally in river banks in northern countries. Little is known on how the riverbank soil temperature responds to air temperature changes and how freeze and thaw develops in a river bank seasonally. This study presents a two-dimensional heat conduction model for numerical investigations of seasonal freeze and thaw processes in an idealized river bank. The model uses the finite difference method and it is convenient for applications. The model is validated with an analytical solution and a field case with soil temperature distributions. It is then applied to the idealized river bank in terms of partially and fully saturated conditions with or without ice cover influence. Simulated results illustrate the response processes of the river bank to seasonal air temperature variations. It promotes the understanding of freeze and thaw processes in river banks and prepares for further investigation of frost and thaw impacts on riverbank stability.

***Keywords*—**Freeze and thaw, river banks, 2D model, heat conduction.

I. Introduction

FREEZE and thaw is one of the most common phenomena appear seasonally in river banks for northern countries in cold regions. In cold periods, the river bank becomes frozen with phase change of pore water in response to low air temperature in saturated soil layers. The frozen bank layers melt gradually when the air temperature increases during the spring. The freeze and thaw processes facilitate river bank retreats and mass collapses by weakening bank materials, cracking of bank slopes, and damaging pavements in canals [1]-[4]. It is well-known that seasonal freeze-thaw affects bank erodibility and stability by reducing the soil strength [5], [6]. The bank erosion and failure due to freeze-thaw effects can be the maximum for the year, especially if the spring high flow occurs during the breakup time.

Existing studies provide useful information in understanding freeze and thaw occurred widely in real fields. Yumoto et al. [7] monitored riverbank profile and freeze and thaw processes at two sites in a small mountain stream, Nikko Volcanic, Japan for twenty months including two winters. Their field observation demonstrated that freeze and thaw triggered notch development and mass failure causing significant subaerial erosion and bank retreats. Kong et al. [8] implemented two piezoceramic-based smart aggregate transducers to quantify soil status in freeze or thaw processes with energy analysis, although the wavelet packet-based soil freeze-thaw status indicator is not linked to soil mechanical properties. In estimation of freeze and thaw depth, the Stefan equation and its corrected versions were widely used by associating freeze and thaw processes with cumulative freezing or thawing air temperature [9]-[12]. However, the Stefan-type equation overestimates the freeze and thaw penetration by ignoring the heat advection and retarded sensible heat. By comprehensive regional investigations of maximum soil freeze depth, soil temperature, climatic and environment changes across China with 845 meteorological stations, Peng et al. [13] found that soil freeze and thaw dynamics were greatly affected by climate changes as maximum soil freeze depth deceased across China with increasing air temperature.

The seasonal air temperature changes play a fundamental role in producing freeze and thaw in the river banks To our best knowledge, it is still challenging to model the frost in river banks caused by seasonal air temperature changes. The objective of this study is to investigate the seasonal freeze and thaw processes in river banks in response to air temperature variations. A two-dimensional heat conduction model is proposed based on the finite difference method. The model is validated with analytical solutions and field observations. By taking an idealized river bank as an example, the model is capable of simulating scenarios of freeze and thaw evolution according to air temperature changes considering the influence of ice cover on the water surface and different saturation conditions.

II. Numerical Algorithm

A river bank might be treated as the two-dimensional problem assuming it is homogeneous in the stream direction for simplicity. Fig. 1 shows half of an idealized trapezoidal cross section representing numerical domain of the bank. The heat conduction equation is used to estimate bank soil temperature changes in response to air temperature variations [9], [14]. In the cold winter, the river bank might suffer phase changes with frozen and unfrozen zones. For the unfrozen zone, there is

$$\rho_u c_u \frac{\partial T}{\partial t} = k_u \left(\frac{\partial^2 T}{\partial y^2} + \frac{\partial^2 T}{\partial z^2}\right) \quad (t > 0, (y, z) \in \Omega_u) \tag{1}$$

Similarly, for the frozen zone,

$$\rho_f c_f \frac{\partial T}{\partial t} = k_f \left(\frac{\partial^2 T}{\partial y^2} + \frac{\partial^2 T}{\partial z^2}\right) \quad \left(t > 0, (y, z) \in \Omega_f\right) \tag{2}$$

in which y = transverse coordinate; z = vertical coordinate; t =

Jiajia Pan is with the State Key Laboratory of Simulation and Regulation of Water Cycle in River Basin, China Institute of Water Resources and Hydropower Research, Beijing 100038, P. R. China (e-mail: panjj@iwhr.com).

time; u, f = subscripts refer to unfrozen and frozen zones; c = specific heat; ρ = soil density; $C = \rho c$ (volumetric heat capacity); k = thermal conductivity; Ω_u = unfrozen zone; Ω_f = frozen zone. Assuming the phase front position is at $S\big(y(t), z(t)\big)$ and the normal direction of the phase front is $\vec{n}$, the energy conservation equation at the interface of frozen and unfrozen layer is

$$k_f \frac{\partial T}{\partial \vec{n}} - k_u \frac{\partial T}{\partial \vec{n}} = L_h \frac{dS\big(y(t),z(t)\big)}{dt} \tag{3}$$

where L_h = latent heat of water. The soil temperature at the phase front is at freezing point T_f, i.e.

$$T(y,z) = T_f \ \big((y,z) \in S(y,z)\big) \tag{4}$$

Equations (1)-(4) can be written in a unified form as [9], [14]

$$\frac{\partial T}{\partial t} = K\left(\frac{\partial^2 T}{\partial y^2} + \frac{\partial^2 T}{\partial z^2}\right) \tag{5}$$

where $K = k/C$ is the unified thermal diffusivity of bank material defined as

$$K = \begin{cases} \frac{k_f}{\rho_f c_f}, & if\ T < T_f - \Delta T \\ \frac{\left\{k_f + \frac{k_u - k_f}{\Delta T}[T - (T_f - \Delta T)]\right\}}{\left\{\rho_f c_f + \frac{w - w_u}{\Delta T} L_h \rho_s\right\}}, & if\ T_f - \Delta T \le T \le T_f \\ \frac{k_u}{\rho_u c_u}, & if\ T > T_f \end{cases} \tag{6}$$

where ΔT = the temperature interval for phase change, usually 1 ℃ [14], [15]; w = total water content; w_u = unfrozen water content; ρ_s = dry bulk soil density; and T_f = freeze temperature of the water. The thermal diffusivity in transition between unfrozen and frozen soil is linearly interpolated according to unfrozen water content and soil temperature [9], [14], [16]. The apparent thermal diffusivity coefficient is used for the soil layer with phase changes assuming the temperature span is ΔT during such conditions.

An explicit finite difference method is applied to solve (5) for its simplicity and efficiency. The discretized equation is

$$T_{i,j}^{n+1} = T_{i,j}^{n} + K\Delta t\left(\frac{T_{i+1,j}^{n} - 2T_{i,j}^{n} + T_{i-1,j}^{n}}{\Delta y^2} + \frac{T_{i,j+1}^{n} - 2T_{i,j}^{n} + T_{i,j-1}^{n}}{\Delta z^2}\right) \tag{7}$$

where i, j = index of transverse and vertical grids; superscripts $n, n+1$ = variables at current and next time steps; Δt = time step; Δy = spatial step in y coordinate; Δz = spatial step in z coordinate.

Fig. 1 shows the numerical domain and boundary conditions at different surfaces. The temperature on the top surface is assumed to be equal to the ambient air temperature. The bank and bed surface temperatures are equal to its ambient temperature of water, ice cover or air which it is exposed to. The temperature at the bottom of the domain is equal to the multiple-years-averaged temperature (T_m).

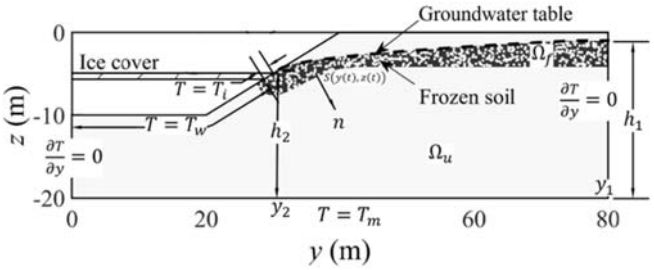

Fig. 1 The idealized river bank and corresponding boundary conditions

Utilizing zero gradient at the symmetric boundary, the second derivation at the left boundary is

$$\frac{\partial^2 T}{\partial y^2} = \frac{\left(T_{2,j}^{n} - T_{1,j}^{n}\right)}{\Delta y^2} \tag{8}$$

Similarly, the discretization on the right boundary is

$$\frac{\partial^2 T}{\partial y^2} = -\frac{\left(T_{ny,j}^{n} - T_{ny-1,j}^{n}\right)}{\Delta y^2} \tag{9}$$

where ny = the grid number at the right boundary. As the explicit method is used, the time step should satisfy the CFL criterion

$$K\Delta t\left(\frac{1}{\Delta y^2} + \frac{1}{\Delta z^2}\right) \le 1 \tag{10}$$

The groundwater table can be described by a parabolic equation based on the Dupuit-Forchheimer formula for seepage flows [17]:

$$\mathrm{h(y)} = \sqrt{\frac{y - y_2}{y_1 - y_2} h_1^2 + \frac{y - y_1}{y_2 - y_1} h_2^2} \tag{11}$$

where h = groundwater table; subscripts 1, 2 are specific locations used as boundaries for the groundwater shown in Fig. 1.

III. Model Validation

Due to the limited data available for soil temperature distributions, the two-dimensional heat conduction model is validated with an analytical solution and a field study. Both cases are essentially one-dimensional problem, and the temperature and soil properties are assumed to be homogeneous in the transverse direction for verifying the two-dimensional model. In validating simulations, the uniform grid is used for both vertical and transverse directions. Ten control cells are used in the transverse direction for efficiency.

A. Validated with Analytical Solutions

Carslaw and Jaeger [18] presented an analytical solution from the semi-infinite theory for the vertical soil temperature changes responding to sinusoidal air temperature variations. Using the annual air temperature at Hanover, New Hampshire, USA as an example, the mean annual temperature is 6.3 ℃ and

the amplitude of the sinusoidal curve is 14.2 ℃. The sinusoidal air temperature is used as top boundary for a homogeneous bank with the height of 10 m. The uniform grid resolution is $0.01\,m$. The soil diffusivity is constantly $1.31E-7\,m^2/s$ assuming no phase change in the bank. Under these conditions, the simulated vertical soil temperature distributions are compared with the analytical solution in Fig. 2. The excellent agreement between them validates the two-dimensional heat conduction model. The range of soil temperature variation becomes smaller going into the deeper layers and the soil temperature remains at a constant value at layers more than 6 m below the top surface. That is because of the energy dissipation and phase delay in heat conduction.

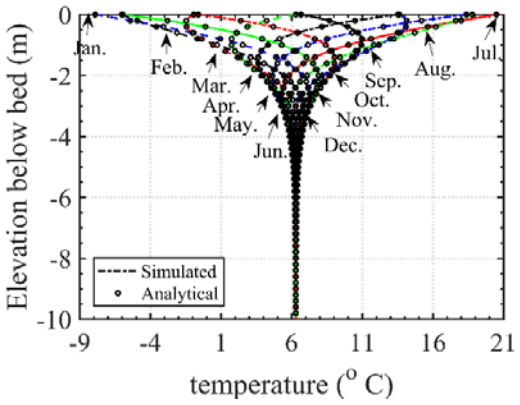

Fig. 2 Simulated and analytical solutions for vertical soil temperature distributions under sinusoidal air temperature variations

B. Validated with Field Observations

The model is then validated with a field observation of bed temperature distribution in Rum River, near Anoka, Minnesota, USA for one month from September 7th to October 7th, 1991 [19]. The grid resolution is 0.0025 m and the soil diffusivity is calibrated to be $1.05E-6\,m^2/s$. The observed soil temperature at 0.1 m and 1.8 m below the surface is used as top and bottom boundaries as shown in Fig. 3. The simulated results are shown in Fig. 4 for soil layers at different locations. The simulated soil temperature history agrees reasonably well with the observations and simulated results from [19].

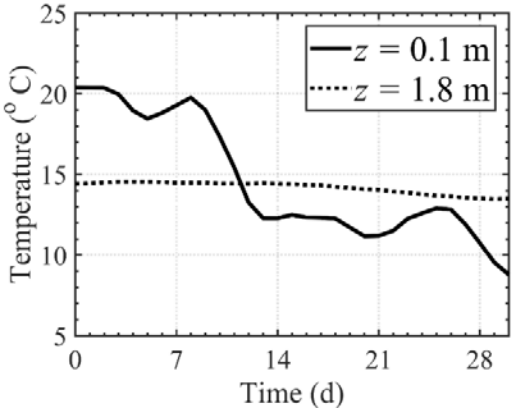

Fig. 3 Top and bottom surface soil temperature history as boundaries

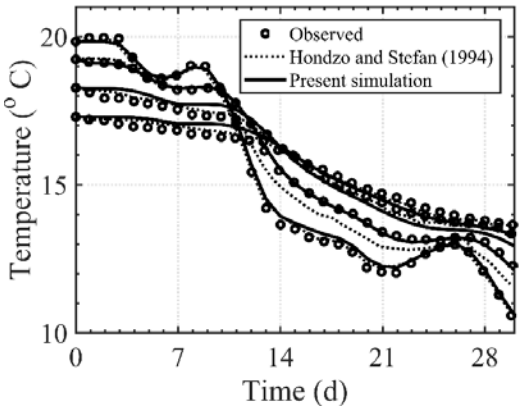

Fig. 4 Simulated and observed soil temperature history compared with simulations of [19] at different locations $z = 0.3\,m, 0.55\,m, 0.8\,m, 1.55\,m$.The initial soil temperature decreases going into deeper soil layers

IV. Model Application

After validation with the analytical solutions and field observations, the two-dimensional heat conduction model is applied to an idealized river bank in examining seasonal freeze and thaw processes and the response processes of soil temperature to air temperature variations. Three field conditions are considered in terms of partially, or fully saturated conditions with or without ice cover impacts. All three cases are based on the domain and boundary conditions shown in Fig. 1.

A. Freeze-Thaw Simulation without Ice Cover

Half of a trapezoidal cross section shown in Fig. 5 with a groundwater table below the top surface of the bank is used for modeling of two-dimensional soil temperature distributions and freeze-thaw in river banks. The width of the numerical domain is 80 m, and the depth is 20 m. The bank height is 10 m with a side slope of 1:2. The groundwater table is estimated by (11) indicated by green dash line in Fig. 5. Taking the air temperature at Hanover, New Hampshire, USA as a reference, the annual air temperature is assumed to follow the sinusoidal curve

$$T_a = 8.8 + 14.2\sin(2\pi ft + 0.1\pi) \tag{12}$$

where $f = \frac{1}{1\,year}$ is the frequency; T_a = air temperature. The water temperature variation follows the air temperature with a lag due to response time needed. Following [20], the water temperature is stated as

$$T_w = \begin{cases} 8.8 + 14.2\cos\alpha\sin(2\pi ft + 0.1\pi - \alpha), & if\ T_w \geq 0; \\ 0, & if\ T_w < 0. \end{cases} \tag{13}$$

where T_w = water temperature; α = the phase shift and it is

$$\alpha = \tan^{-1}\frac{2\pi f}{k_r} \tag{14}$$

where k_r = response parameter. Based on (12) and (13), the variation of air temperature and water temperature is shown in

Fig. 7 taking $k_r = 0.093$ and $\alpha = 0.17$ as an example. The water temperature is truncated at 0 ℃ during the freezing period. Taking these water and air temperature into boundary conditions shown in Fig. 1, the two-dimensional heat conduction model is applied to simulate freeze and thaw processes in the river bank in terms of no ice cover conditions. The spatial step is 0.1 m, while the time step is 3600 s. Soil properties are listed in Table I using peaty clay and sand in the Beiluhe basin of Qinghai-Tibet Plateau as an example [21].

Taking (12) and (13) as surface boundary for 10 years' simulations, the soil temperature distribution becomes stable in the whole domain. The stabilized temperature distribution on July 1st is used as the initial condition as shown in Fig. 5. The seepage surface is assumed to start at $(y_1 = 80\ m, z_1 = -1\ m)$ and terminate at $(y_2 = 30.9\ m, z_2 = -4.5\ m)$. The river water surface is located at $z = -5\ m$.

TABLE I
SOIL PROPERTIES UNDER FROZEN AND UNFROZEN CONDITIONS (AFTER [21])

Frozen thermal conductivity	Unfrozen thermal conductivity	Frozen volumetric heat capacity	Unfrozen volumetric heat capacity	Frozen soil density	Unfrozen soil density	Unsaturated soil density	Total water content	Unfrozen water content	Latent heat
k_f	k_u	C_f	C_u	ρ_f	ρ_u	ρ	w	w_u	L
W/m℃	W/m℃	J/m^3℃	J/m^3℃	kg/m^3	kg/m^3	kg/m^3	kg/kg	kg/kg	J/kg
2.12	1.36	2.54E+6	3.45E+6	1400	1450	1420	50	4.80	3.34E+5

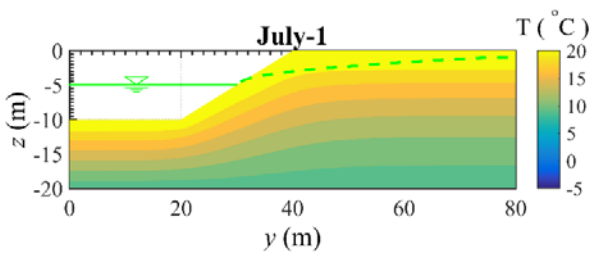

Fig. 5 Soil temperature distribution on July 1 used as the initial condition

Fig. 6 shows simulated results of the annual cycle of soil temperature distributions and phase changes from August to June. The dark blue zone with white particles under the groundwater table represents frozen zone in the river bank when the soil temperature goes below 0 ℃ and it is labelled as the same in Figs. 8 and 9. In August, the soil temperature varies from 9 ℃ to 22 ℃ in the bed. The temperature decreases gradually from the top to bottom. The soil temperature cools down as air temperature decreases from August to January. In November, the air temperature goes below 0 ℃ and the water temperature remains at 0 ℃ as indicated by Fig. 7. The temperature of river bank and the bed exposed to water remains at 0 ℃ while the temperature of bank surface exposed to cold air goes below −0 ℃. Due to the insulation effects of water in the cross section, a small frozen zone appears near the water surface. Compared to that in October, the soil temperature is colder in the domain and the temperature increases going to deeper layers. That is reasonable as the top boundary temperature becomes lower than that in the deeper soil layer where it is remains at constant. The frozen zone grows a little in December as the surface air temperature becomes lower, while the cold zone in the river bank goes deeper than that in November. Besides, significant growth of frozen area occurs along the seepage surface. In January, the frozen zone in the river bank continually grow as the air temperature reaches the lowest of the year. The air temperature increases after February, and the frozen zone in the bank starts to decrease. In March, both the air and water temperatures go above freezing point, and the frozen zone in the bank disappears. The surface layer becomes warmer in response to the higher boundary temperature while the deeper layer remains at the long-term averaged air temperature. During the whole winter, the river bed underneath the water is significantly warmer than bank area exposed to the cold air. That is because the water temperature remains at the freezing point and protects the river bed from low air temperature effects. It should be noted that no frozen appears above the groundwater table because of unsaturated condition there.

B. Freeze-Thaw Simulation with Ice Cover

Using the same domain, air temperature and water temperature boundaries, the model is further applied to the idealized bank considering ice cover formation and melting processes. The ice cover is assumed to appear on November 15th when water temperature is at the freezing point. The ice cover thickness is calculated by the freezing-degree-day formula:

$$h_i = \alpha_f \{\sum_{t=0}^{N} [-T_a \Delta t]\}^{1/2} \quad (15)$$

where h_i = ice cover thickness, cm; T_a = daily-averaged air temperature, ^{0}C; $\alpha_f = 1.5\ cm\ ℃^{-1/2} day^{-1/2}$ for typical river ice covers [22]; and $\Delta t = 1\ day$. The top of ice cover is at $z = -5 + 0.1 h_i\ (m)$ and the bottom of ice cover is at $z = -5 - 0.9 h_i\ (m)$, with water surface located at $z = -5\ m$. For simplicity, the ice cover is assumed to have temperature linearly distributed from its top to bottom and it melt out when the air temperature goes above the freezing point. The average ice cover temperature history is shown in Fig. 7 along with water temperature and air temperature variations. The existence of ice cover lasts from November to February and thus it impacts soil temperature and frozen zone in these periods.

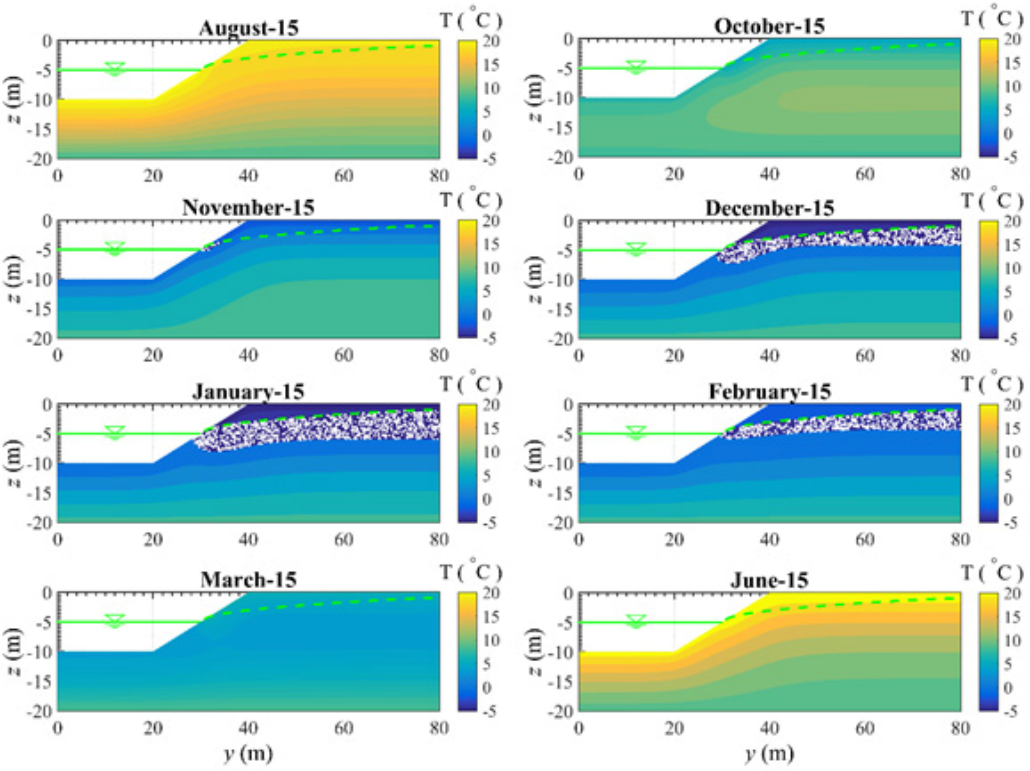

Fig. 6 Simulated soil temperature distributions and frozen zone in the river bank

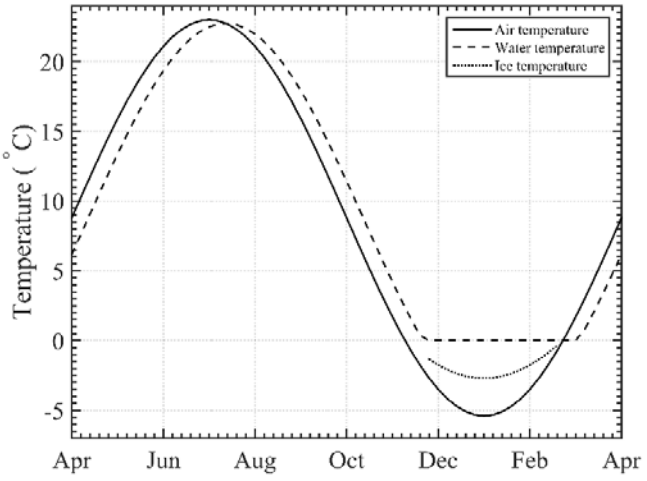

Fig. 7 Air temperature and corresponding water and ice cover temperature

Fig. 8 shows the annual cycle of soil temperature distributions and the frozen zone variations from October to March. In periods without ice cover from March to October, the simulated soil temperature distributions are the same as these in Fig. 6. In comparison to simulated results without ice cover, Fig. 8 shows that the area of the frozen layer is larger and the frozen layer goes deeper below the water surface during the ice cover influence periods. That is because the temperature of bank surface in contact with the ice cover can go below 0 ℃ instead of remaining at the freezing point. The existence of ice cover extends the exposure of bank surface to cold ambient temperature.

C. Freeze-Thaw Simulation with Fully Saturated Bank and Ice Cover

Using the same domain and boundary conditions as stated in Section IV *B*, the model is applied to the idealized bank in fully saturated situations to investigate the influence of different saturation on freeze and thaw changes. Fig. 9 shows the seasonal variations of soil temperature and frozen zone in response to air temperature changes with fully saturated bank and ice cover. The frozen zone with phase change starts from the top bank surface and extends to deeper layer as ambient temperature becomes lower. That is because the whole domain is fully saturated and the soil layer might become frozen whenever its temperature goes below the freezing point. The phase change starts to appear from the top bank surface in November. The area of frozen zone reaches its maximum in January, when the air temperature reaches its minimum. The area of frozen zone decreases as the soil temperature warms up in deeper layers in February. Since the air temperature still remains below freezing the ice cover thickness continue to increase at that time. In March, the ice cover melts out and the frozen layer disappears as soil temperature goes above freezing point. In comparison with other two cases, Fig. 9 shows larger area of frozen zone in the winter, because the frozen soil layer initiates from the bank surface exposes to the cold ambient environment.

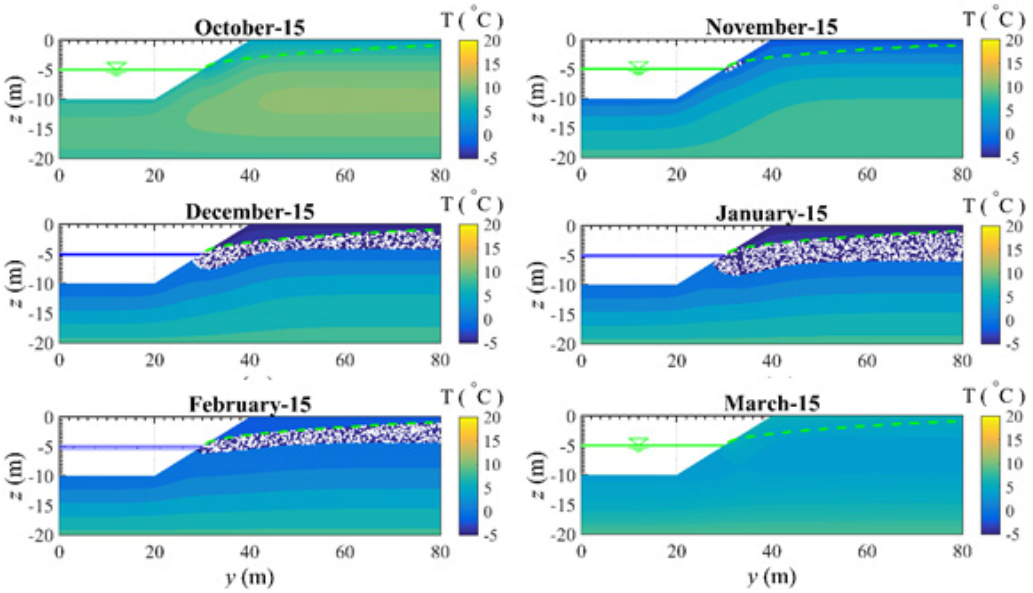

Fig. 8 Simulated soil temperature distributions and frozen zone in the river bank

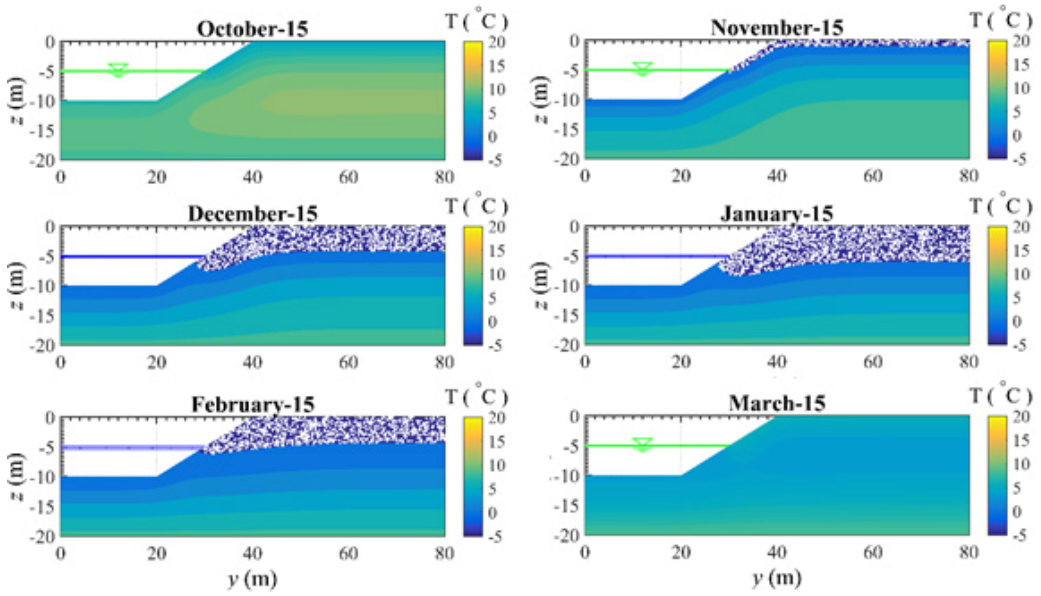

Fig. 9 Simulated soil temperature distribution and frozen layer in the river bank

V. Discussions

Case studies with and without ice cover influence show that the ice cover appearance causes larger cold exposure area in the cross-sectional bank surface and thus results in larger frozen zone. The difference of simulated freeze and thaw processes is small between cases with and without ice cover. That is because the maximum ice cover thickness is about 0.8 m and its influence area is small compared to bank surface longer than 100 m exposed to cold air. The fully saturated bank suffers more serious freeze and thaw influence. It has larger frozen area with phase change in the saturated bank because of sufficient pore water available from bank surface to deeper layers. The bank materials become frozen as long as the soil temperature goes below the freezing point.

The two-dimensional heat conduction equation is used to represent soil energy transport processes by ignoring advection processes of heat exchange from groundwater flow. In most situations, the energy transfer from mass changes between open channel flow and groundwater is negligible. Thus, it is reasonable to use heat conduction equation to illustrate the main heat transfer mechanics in river banks. For uniform channel with gradual varied flow, the three-dimensional heat conduction equation is simplified to the existing two-dimensional formulation shown in (5). Besides, bank soil properties are assumed to be homogeneous in the idealized case study for simplicity. In real field study, soil properties can vary at different soil layers and the existing model might be extended for such conditions by using different soil diffusivity and bulk

densities for different soil layers. The model represents the most dominant heat conduction processes in the river bank.

Freeze and thaw is a key factor of weathering and weakening processes for river banks resulting in high risks of bank slope failure and mass erosion. Freeze and thaw processes decrease the effective shear stress of soil and the frictional strength during frost heave and thaw consolidation [5], [23]-[26]. In the frost heaving processes, the soil structure is destroyed and ice heaves soil particles decreasing inter-particle friction. During the thaw consolidation, the pore water pressure accumulates rapidly in the ice-rich bank layers resulting in oversaturated conditions. Such high pore water pressure might result in downslope seepage in the streambanks and facilitate the bank retreats and mass erosions. That is why most bank retreats and slope failures occur in winter months of December, January, and February due to destroy soil structure, weakened shear strength, and decreased soil cohesion related to frozen and thaw processes [27]-[32].

VI. Conclusions

This study presents a two-dimensional heat conduction model based on the unified conduction equations for frozen and unfrozen soil with phase changes. The model is validated with soil temperature data from an analytical solution and field observations. Their good agreement verifies the capability of the model. It is further applied to simulate freeze and thaw processes in response of air temperature changes in an idealized river bank in partially, or fully saturated conditions with or without ice cover influence. The existence of ice cover extends exposed area of bank surface to cold ambient temperature and results in larger frozen zone in December, January and February. The frozen zone with phase changes is significantly larger in fully saturated condition than that in partial saturation. The freeze and thaw processes are closely related to ambient air, water and ice cover temperature changes to which the bank surface is exposed. The study illustrates frozen zone changes in an idealized river bank and prepares for further investigations of frozen and thaw influence on bank erosions frequently occurs in later winter and early spring.

Acknowledgment

We appreciate the financial support from the Second Tibetan Plateau Scientific Expedition and Research Program (2019QZKK020706), and the National Natural Science Foundation of China (51979291, 52009144).

References

[1] Zhang, Z.X. and R.L. Kushwaha, Modeling soil freeze-thaw and ice effect on canal bank. Canadian Geotechnical Journal, 1998. 35(4): p. 655-665.
[2] Thomas, H.R., et al., Modelling of cryogenic processes in permafrost and seasonally frozen soils. Geotechnique, 2009. 59(3): p. 173-184.
[3] Li, Z., et al., Numerical study on the effect of frost heave prevention with different canal lining structures in seasonally frozen ground regions. Cold Regions Science and Technology, 2013. 85: p. 242-249.
[4] Li, S., et al., Moisture–temperature changes and freeze–thaw hazards on a canal in seasonally frozen regions. Natural Hazards, 2014. 72(2): p. 287-308.
[5] Gatto, L.W., Soil Freeze-Thaw Effects on Bank Erodibility and Stability. 1995, DTIC Document.
[6] Kimiaghalam, N., et al., A comprehensive fluvial geomorphology study of riverbank erosion on the Red River in Winnipeg, Manitoba, Canada. Journal of Hydrology, 2015. 529: p. 1488-1498.
[7] Yumoto, M., et al., Riverbank freeze-thaw erosion along a small mountain stream, Nikko volcanic area, central Japan. Permafrost and Periglacial Processes, 2006. 17(4): p. 325-339.
[8] Kong, Q., et al., Monitoring the soil freeze-thaw process using piezoceramic-based smart aggregate. Journal of Cold Regions Engineering, 2014. 28(2): p. 971-984.
[9] Lunardini, V.J., Heat transfer in cold climates. 1981: Van Nostrand Reinhold Company.
[10] Woo, M.K., et al., A two-directional freeze and thaw algorithm for hydrologic and land surface modelling. Geophysical Research Letters, 2004. 31(12).
[11] Yi, S., M.A. Arain, and M.K. Woo, Modifications of a land surface scheme for improved simulation of ground freeze-thaw in northern environments. Geophysical Research Letters, 2006. 33(13).
[12] Kurylyk, B.L. and M. Hayashi, Improved Stefan equation correction factors to accommodate sensible heat storage during soil freezing or thawing. Permafrost and Periglacial Processes, 2016. 27(2): p. 189-203.
[13] Peng, X., et al., Response of seasonal soil freeze depth to climate change across China. Cryosphere, 2017. 11(3).
[14] Ling, F. and T. Zhang, Numerical simulation of permafrost thermal regime and talik development under shallow thaw lakes on the Alaskan Arctic Coastal Plain. Journal of Geophysical Research: Atmospheres, 2003. 108(D16).
[15] Comini, G., et al., Finite element solution of non-linear heat conduction problems with special reference to phase change. International Journal for Numerical Methods in Engineering, 1974. 8(3): p. 613-624.
[16] Osterkamp, T., Freezing and thawing of soils and permafrost containing unfrozen water or brine. Water Resources Research, 1987. 23(12): p. 2279-2285.
[17] Bear, J., Hydraulics of groundwater. 2012: Courier Corporation.
[18] Carslaw, H. and J. Jaeger, Conduction of heat in solids. Vol. 19591. 1959: Clarendon Press, Oxford.
[19] Hondzo, M. and H.G. Stefan, Riverbed heat conduction prediction. Water Resources Research, 1994. 30(5): p. 1503-1513.
[20] Foltyn, E.P. and H.T. Shen, St. Lawrence River freeze-up forecast. Journal of Waterway, Port, Coastal, and Ocean Engineering, 1986. 112(4): p. 467-481.
[21] Ling, F., et al., Modelling open-talik formation and permafrost lateral thaw under a thermokarst lake, Beiluhe Basin, Qinghai-Tibet Plateau. Permafrost and Periglacial Processes, 2012. 23(4): p. 312-321.
[22] Michel, B., Winter Regime of Rivers and Lakes. Cold Regions Science and Engineering Monograph III-Bla. US Army, Corps of Engineers, 1971.
[23] Lawson, D.E., Erosion of perennially frozen streambanks. 1983, DTIC Document.
[24] Nicholson, D.T. and F.H. Nicholson, Physical deterioration of sedimentary rocks subjected to experimental freeze–thaw weathering. Earth Surface Processes and Landforms, 2000. 25(12): p. 1295-1307.
[25] Ji-Lin, Q. and M. Wei, State-of-art of research on mechanical properties of frozen soils. Rock and Soil Mechanics, 2010. 31(1): p. 133-143.
[26] Cui, Z.-D., P.-P. He, and W.-H. Yang, Mechanical properties of a silty clay subjected to freezing–thawing. Cold Regions Science and Technology, 2014. 98: p. 26-34.
[27] Wolman, M., Factors influencing erosion of a cohesive river bank. American Journal of Science, 1959. 257(3): p. 204-216.
[28] Gardiner, T., Some factors promoting channel bank erosion, River Lagan, County Down. Journal of Earth Sciences, 1983. 5(2): p. 231-239.
[29] Lawler, D., River bank erosion and the influence of frost: a statistical examination. Transactions of the Institute of British Geographers, 1986. 11(2): p. 227-242.
[30] Englehardt, B. and K. Waren, Upper Missouri River bank erosion. Unpublished report, North Dakota State Water Commission, Bismarck, and Montana Department of Natural Resources and Conservation, Helena, 1991.
[31] Couper, P.R., Space and time in river bank erosion research: A review. Area, 2004. 36(4): p. 387-403.
[32] Pollen, N. and A. Simon, Estimating the mechanical effects of riparian vegetation on stream bank stability using a fiber bundle model. Water Resources Research, 2005. 41(7).